

Structural complexity and phonon physics in 2D arsenenes

Jesús Carrete

Institute of Materials Chemistry, TU Wien, A-1060 Vienna, Austria

E-mail: jesus.carrete.montana@tuwien.ac.at

Luis J. Gallego

Departamento de Física de la Materia Condensada, Facultad de Física, Universidad de Santiago de Compostela, E-15782 Santiago de Compostela, Spain

Natalio Mingo

Université Grenoble Alpes, F-38000 Grenoble, France

CEA, LITEN, 17 rue des Martyrs, F-38054 Grenoble, France

Abstract. Using ab-initio lattice dynamics, we find a finite-temperature stability crossover of three arsenene phases, contrasting with previous publications, and we prove that a fourth phase found in the literature turns out to be mechanically unstable. Furthermore, our results also challenge the common assumption of an inverse correlation between structural complexity and thermal conductivity. Instead, a richer picture emerges from our results, showing how harmonic interactions, anharmonicity and symmetries all play a role in modulating thermal conduction in arsenenes. More generally, our conclusions highlight how vibrational properties are an essential element to be carefully taken into account in theoretical searches for new 2D materials.

1. Introduction

After the first experimental isolation and electronic characterization of graphene [1], whose band structure had earlier been analyzed by Wallace [2], and subsequently by Reich et al. [3], growing interest has been devoted to the properties of two-dimensional (2D) nanostructures. Significant advances have been achieved by means of theoretical predictions and the successful synthesis and characterization of new single- and few-layer materials, very often in that order due to the difficulties of nanoscale experimental measurements. Due to the peculiar physical and chemical properties owing to their low dimensionality, 2D nanostructures have a huge diversity of potential applications in nanoelectronics, spintronics, optoelectronics, fabrication of high-performance electrodes, hydrogen storage devices, nanotribology and nanomedicine, among other fields [4–16]. The number of already synthetized or predicted 2D materials is increasing continuously, and it is expected that in the next few years a new generation of 2D materials will be available alongside a complete and accurate characterization of their properties.

The zero band gap of 2D phases of group-IV elements such as graphene [1], silicene and germanene [17] places constraints on their potential technological use, specifically in the field of optoelectronics. Although the band gap can be opened by doping with particular species [18–20] or by applying an external electric field [21, 22], this fact has spurred recent interest in other 2D materials. In particular, great attention has been devoted to those derived from group-V elements. Black phosphorene (a single layer of black phosphorous) was investigated early on [23], and it was found that the single layer has a much wider band than the bulk phase (~ 2 eV vs. ~ 0.34) [24]. The structure of black phosphorene is puckered, rather than flat (as graphene) or buckled (as silicene). However, buckled phosphorene, called blue phosphorene, was also predicted to be stable by first-principles calculations [25]. Subsequent theoretical calculations by Zhang et al. [26] showed that 2D honeycomb structures of As and Sb (arsenene and antimonene), which are semimetals in bulk forms, are indirect semiconductors with band gaps of 2.49 and 2.28 eV, respectively, which can be useful for optoelectronic devices working under blue or UV light. Moreover, they undergo indirect-direct band-gap transitions under small amounts of biaxial strain, which is a clear advantage for their use in optoelectronics, as electronic excitations are feasible with lower photon energies.

Almost at the same time, Kamal and Ezawa [27] theoretically showed that two types of arsenene structures, buckled and puckered, are stable and that they possess strain-tunable indirect band gaps. Extensive theoretical calculations of the mechanical and electronic properties of nitrogen [28], arsenene [29], antimonene [30] and bismutene [31] have recently been performed by Ciraci and coworkers that, alongside the previous studies on phosphorene [23–25], complete a picture of these properties for group-V 2D materials. It should be noted that phosphorous, arsenic, antimony and bismuth form quasi-layered 3D crystals, which justifies the efforts to explore and synthesize group-V monolayers.

A fundamental element in all these theoretical inquiries has been the stability of the predicted monolayers. Two aspects of this question are whether the structure is stable with respect to small perturbations (mechanical stability) and whether there are competing 2D structures which are thermodynamically favored. The first aspect has been investigated by calculating the phonon spectra using standard ab initio methods and, sometimes, also by finite-temperature ab initio molecular dynamics (MD) simulations (see, for instance, Refs. 29 and 32). Regarding the assessment of thermodynamic stability, it is typically based on an accurate determination of the energy per atom of each structure from first principles. However, this approximation neglects the contribution of phonons to the free energy, which even at zero temperature can change the energetic ordering of two structures. Moreover, in both cases the conclusions are often compromised by a failure to enforce the fundamental rotational invariance of mechanics upon the phonon dispersions [33], which has negligible importance for bulk crystals but is critical in 2D materials.

In the case of arsenene, one of the group-V 2D materials investigated in more detail so far, two different structures were originally proposed [26, 27, 29]: a buckled honeycomb structure and a puckered structure (also known as a symmetric washboard structure [29]). However, very recently two new candidate structures have been put forward: a tricycle structure [34], and a structure consisting of buckled square and octagon rings [32]. Both have been predicted to be direct-band-gap semiconductors, the former with an energy gap of 1.38 eV and the latter with an appreciable band gap whose estimated value depends on the exchange and correlation functional employed in the calculations [32]. Multilayer arsenene nanoribbons have already been synthesized on an InAs substrate using the plasma-assisted process, and the band gap has been estimated to be about 2.3 eV [35]. All four structures are depicted in Fig. 1.

The overall theoretical description of arsenene has recently been supplemented with two studies on its thermal transport [36, 37]. Just like both of the aforementioned aspects of stability, the thermal conductivity of semiconductors is determined by the physics of phonons in the material. Investigation of this property in 2D materials in general is of paramount importance not only for theoretical reasons (the desire to understand how thermal transport behaves in this dimensionality) but also with a view to practical applications such as heat dissipation in nanoelectronics. In the first of those published studies, Zeraati et al. [36] focused their attention on the puckered structure

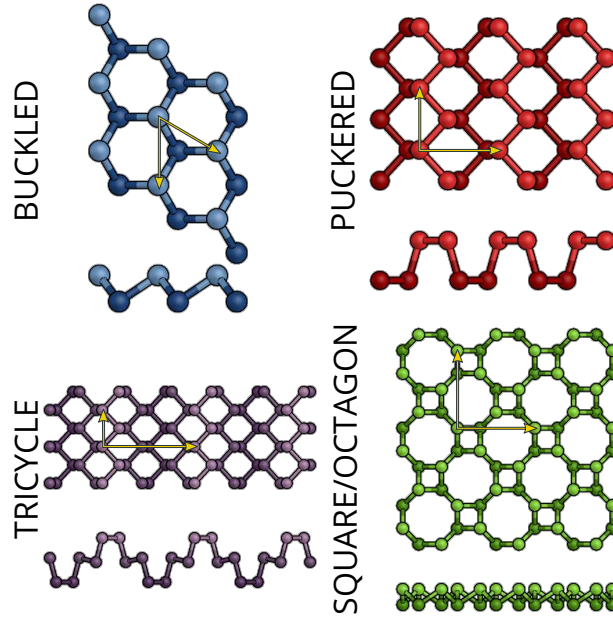


Figure 1. Top and side views of a 3×3 supercell of each of the arsenene structures considered in this paper. The superimposed arrows represent the unit cell vectors.

of arsenene, finding a very anisotropic room-temperature thermal conductivity of 30.4 and 7.8 W/ (m K) along the zigzag and armchair directions, respectively. In the second one, Zheng et al. [37] made a comparative study of the thermal conductivity of the buckled and puckered structures, confirming that the former is isotropic while the latter is anisotropic. Both of these studies on the thermal conductivity of arsenene were performed using standard ab-initio methods and the ShengBTE package for solving the Boltzmann transport equation for phonons [38]. However, inspection of their computed phonon spectra reveals the possible absence of the rotational symmetry in the force constants, which can have a strong influence on the predicted thermal conductivities (to the point of reversing the estimated anisotropy) as demonstrated for the case of borophene [33]. Specifically, this symmetry manifests itself in the presence of a ZA branch that is perfectly quadratic close to the Γ point; any finite group velocity there is a sign of a violation.

In the work described here we perform a first-principles study of the equilibrium structures and lattice dynamics of the four possible phases of arsenene represented in Fig. 1: buckled, puckered, tricycle and square/octagon (s/o). We find that the tricycle phase is mechanically unstable, so we discard it for further study. The remaining structures are found to be stable, although the spectra of the buckled and puckered phases differ from those previously reported [26, 27, 29, 36, 37]. More importantly, we show that inclusion of phonons in the energetic picture turn the puckered and s/o structures into the most stable ones at low and room temperatures, respectively. This contradicts previous analyses based on ground-state energies alone, which predict the buckled structure as the most stable one. We also study thermal transport in all four

Table 1. Main geometric features and cohesive energies of the four arsenene structures after relaxation.

structure	space group	lattice parameters (Å)	atoms / unit cell	bond lengths (Å)	frozen-nuclei cohesive energy (eV/atom)	zero-point harmonic energy (eV/atom)
buckled	P $\bar{3}$ m1	3.607	2	2.508	2.963	2.763
puckered	Pmna	3.686, 4.754	4	2.492, 2.514	2.926	2.711
tricycle	Pbcm	3.646, 9.543	8	2.500, 2.512	2.947	unstable
s/o	P4/nbm	7.126	8	2.504, 2.525	2.862	2.699

structures, and show a lack of a simple correlation between unit-cell complexity and thermal conductivity.

2. Results and discussion

We start by performing a local relaxation of each structure using the density functional theory (DFT) package VASP [39–42] with projector-augmented-wave (PAW) datasets [43, 44] and the Perdew-Burke-Ernzerhof (PBE) approximation to exchange and correlation [45, 46]. We employ a 40×40 Γ -centered regular grid to sample reciprocal space, and a cutoff energy of 261 eV, which afford fully converged results in all cases. Our unit cells span 25 Å in the through-plane directions of the layers to avoid spurious interactions due to the periodic boundary conditions. The main geometric features obtained from the relaxation are summarized in Table 1 along with their cohesive energies per atom, defined as the difference between the energy of an isolated As atom and the average energy per atom in the structure.

Our geometric results for the buckled, puckered and s/o structures agree quite well with the results reported in Ref. 32, although our cohesive energies are slightly lower. Likewise, the geometry we obtain for the tricycle structure is in fair agreement with that reported in Ref. 34, and its energetics place it between the buckled and puckered structures.

Our next step is to calculate the phonon dispersions for each structure using a real-space method. We use Phonopy [47] to create a minimal set of displaced supercell configurations and again VASP to compute the forces induced by those displacements. We choose supercell sizes of 9×9 , 7×7 , 5×5 and 5×5 for the buckled, puckered, tricycle and s/o structures respectively, which afford converged phonon dispersions using Γ -point-only DFT runs. After obtaining a set of “raw” DFT-based force constants, we correct them using the procedure presented in Ref. 33 to remove any violation of the translation and rotation symmetries of free space. The resulting phonon dispersions and vibrational densities of states are shown in Fig. 2.

All four spectra show an energy gap between a group of high-energy, rather localized, optical modes and the remaining (acoustic plus optical) phonon branches,

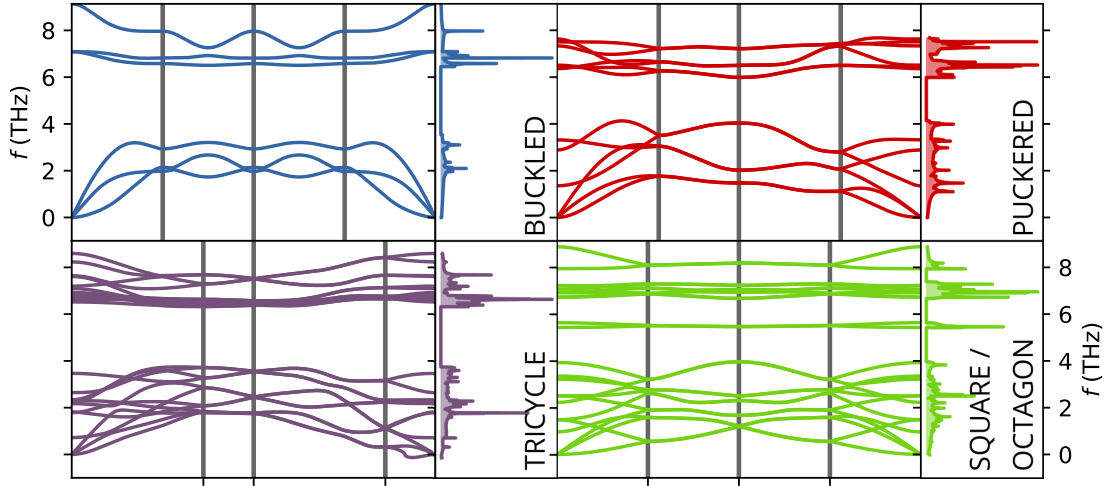


Figure 2. Phonon dispersions and normalized vibrational densities of states for the four phases of arsenene studied in this work. In each case the bands are plotted along the path $\Gamma \rightarrow (1/2, 0) \rightarrow (1/2, 1/2) \rightarrow (0, 1/2) \rightarrow \Gamma$ in the respective reduced reciprocal coordinates.

a general feature of 2D arsenenes according to the literature [26, 27, 29, 32, 36, 37] with the only exception of Ref. 34, which introduces the tricycle structure. In fact, our predicted spectrum for the tricycle phase is completely different from the one included in Ref. 34; in particular, it is the only phase for which we predict imaginary frequencies (represented as real and negative in Fig. 2, as is conventional). This is the fingerprint of mechanical instability, pointing to a family of spontaneous deformations of the structure towards a lower-energy configuration. The instability extends more than halfway from Γ to $(0, 1/2)$ and through several points that are commensurate with the 5×5 supercell and is resilient against changes in supercell size, making it unlikely that it be a numerical effect. Therefore, even though we find the cohesive energy of the tricycle phase to be the next-to-lowest one (Table 1), this phase cannot be considered as stable, and is not included in our remaining calculations.

Another reason to question the reliability of the spectrum for the tricycle phase given in Ref. 34 is the non-zero group velocity of the convex phonon branch close to Γ . Unfortunately this feature is shared with most published spectra, pointing to mild [36] or serious [26, 27, 29, 37] violations of the fundamental isotropy of free space in the calculations. Only the authors of Ref. 32 seem to have enforced full rotational symmetry. As noted in previous studies [33, 48], this can make the difference between a fully stable spectrum and one containing artifactual imaginary frequencies. This could also be the reason for the prediction of buckled arsenene as unstable in Ref. 27.

Equipped with these phonon spectra, we improve our estimate of the total energy of each structure at 0 K beyond the frozen-nuclei approximation by including the ground-

state energy of each vibrational mode:

$$E = E_{\text{frozen}} + \frac{h}{2} \sum_{\lambda} f_{\lambda}. \quad (1)$$

Here h is the Planck constant, and f_{λ} is the frequency of the vibrational mode labeled by λ , an index comprising both a point \mathbf{q} in reciprocal space and a branch index α . The sum \sum_{λ} denotes both a literal sum over α and an average over the Brillouin zone by means of an integral in \mathbf{q} . This correction, whose values we show in Table 1, is enough to change the ordering of the energies. Our improved predictions for the cohesive energy of the three stable phases are 0.200 eV/atom (buckled), 0.216 eV/atom (puckered) and 0.163 eV/atom (s/o). Therefore the most stable phase at vanishing temperature is the puckered structure, and not the buckled one.

We complete the quasiharmonic study of the stability of 2D arsenenes by computing the full quasiharmonic free energy, obtaining by adding the temperature-dependent energy and entropy terms to Eq. (1):

$$\begin{aligned} F &= E_{\text{frozen}} + E_{\text{vib}}(T) - TS_{\text{vib}}(T) = \\ &= E_{\text{frozen}} - \frac{h}{2} \sum_{\lambda} f_{\lambda} - k_B T \sum_{\lambda} \log n_{\lambda}(T), \end{aligned} \quad (2)$$

where $n_{\lambda}(T) = \left[1 - \exp\left(\frac{hf_{\lambda}}{k_B T}\right)\right]^{-1}$ is the Bose-Einstein occupancy factor of mode λ at temperature T (k_B is the Boltzmann constant). The results are plotted in Fig. 3 with respect to the free energy of the buckled phase at each temperature. As can be seen in the figure, there is a crossover around 60 K that suggests that the square/octagon phase recently proposed by Ciraci and coworkers [32] may be the thermodynamically favored one at room temperature.

We now focus our attention on the lattice thermal conductivity tensor of each structure. Under the relaxation-time approximation to the Boltzmann transport equation for phonons, it can be computed as

$$\kappa^{(\mu\nu)} = \frac{1}{k_B T^2 A} \sum_{\lambda} n_{\lambda} (n_{\lambda} + 1) (hf_{\lambda})^2 v_{\lambda}^{(\mu)} v_{\lambda}^{(\nu)} \tau_{\lambda}. \quad (3)$$

Here, μ and ν are Cartesian indices, A is the area of the unit cell, \mathbf{v}_{λ} is the group velocity of mode λ , and τ_{λ} its relaxation time. We note that with this definition the S.I. units of κ are W K^{-1} instead of the more typical $\text{W m}^{-1} \text{K}^{-1}$. This convention is better suited for 2D systems, where heat flux is defined per unit length, and not per unit area. It avoids the conceptually unpleasant difficulty of having to introduce an artifactual and ambiguous thickness for the 2D layer, and allows for easier comparison between different 2D systems.

It remains to compute the relaxation time in Eq. (3). In the absence of crystalline defects, the dominant source of phonon scattering is anharmonicity, whose leading term can be characterized by the full set of third-order derivatives of the potential energy, i.e.,

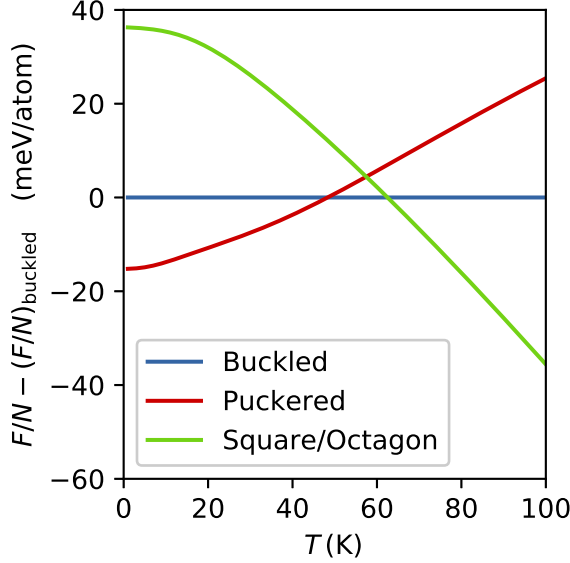


Figure 3. Relative quasiharmonic free energies of the three stable phases of arsenene studied in this work, as a function of temperature. The free energy of the buckled phase at each temperature is chosen as the reference.

the third-order force constants. This is particularly true for arsenic, as this element has only one stable isotope and hence lacks any contribution to phonon scattering from mass disorder [49], allowing us to better focus on anharmonicity. We generate a minimal set of supercell configurations required to obtain all those constants, we obtain the forces on atoms in those configurations using VASP with the same parameters as for the harmonic calculations, and we rebuild the third-order force-constant tensor, compute the anharmonic scattering rates, and thus obtain κ from first principles using the AlmaBTE software package [50], following the procedure described in detail in Ref. 38.

To analyze the harmonic and anharmonic contributions, we also compute the reduced thermal conductivity [51]:

$$\tilde{\kappa}^{(\mu\nu)} = \frac{1}{k_B T^2 A} \sum_{\lambda} n_{\lambda} (n_{\lambda} + 1) (h f_{\lambda})^2 \frac{v_{\lambda}^{(\mu)} v_{\lambda}^{(\nu)}}{|\mathbf{v}_{\lambda}|}. \quad (4)$$

If every heat carrier in the system had the same mean free path $\Lambda = |\mathbf{v}_{\lambda}| \tau_{\lambda}$, κ would become proportional to Λ . The proportionality constant would be $\tilde{\kappa}$, which can hence be interpreted as a purely harmonic descriptor of the effect of phonon frequencies and group velocities on the thermal conductivity when anharmonicity is homogenized in a particular way.

It is easy to see, based on symmetry considerations, that the buckled and s/o arsenene monolayers are isotropic, so their thermal conductivity can be treated as a scalar. The puckered layer, in contrast, has two independent thermal conductivities corresponding to the nonequivalent zigzag and armchair directions.

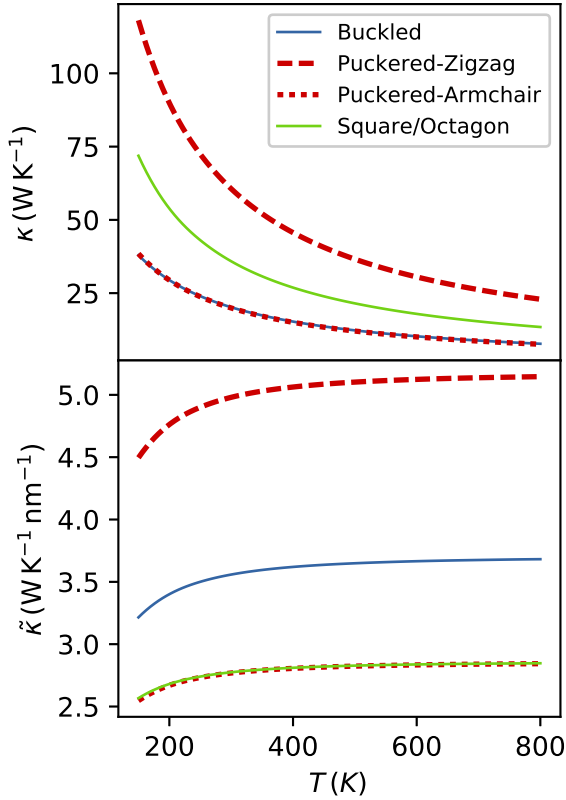


Figure 4. Thermal conductivity (top) and reduced thermal conductivity (bottom) for the three stable phases of arsenene studied in this work, as a function of temperature.

The independent components of κ and $\tilde{\kappa}$ are shown in Fig. 4. These results confirm the highly anisotropic character of the puckered phase of arsenene with regard to thermal transport, first reported in Ref. 36. More remarkably, they show that the buckled phase conducts heat more poorly than any of the other options; indeed, the room-temperature thermal conductivity of the puckered phase along the fast zigzag axis is three times higher than that of the buckled phase. This observation flies in the face of the intuitive trend that to maximize lattice thermal conductivity one should look for simple structures, with high band degeneracy and hence few possible phonon scattering router. Here, even the 8-atom-per-unit-cell s/o structure displays roughly twice the room-temperature thermal conductivity of the simpler buckled phase.

A good understanding of the factors determining whether a material is a good or a bad thermal conductor is critical for materials discovery initiatives looking for innovative solutions to heat dissipation problems. Hence we take a deeper look at the reasons for the counter-intuitive ordering of the thermal conductivities of arsenenes. The bottom panel in Fig. 4 gives a hint that the causes behind the high thermal conductivity of the two more complex phases are different. Specifically, the reduced thermal conductivity of puckered arsenene in the zigzag direction is already much higher than that of the

buckled phase, but the value for the s/o structure is actually much lower. In other words, harmonic effects are responsible for the high conductivity of the puckered structure. In the s/o structure, however, a reduced anharmonicity plays the key role in preventing κ from falling much lower.

Regarding the puckered phase, the favorable harmonic contribution to thermal transport may be due to the low-lying optical branches with relatively high average velocities in the direction of reciprocal space corresponding to the short axis of the puckered-arsenene unit cell. (Fig. 2, top-right panel). As for the s/o phase, a low reduced thermal conductivity is to be expected given the generally low group velocities of low-frequency phonons (Fig. 2, bottom-right panel), while the low scattering rates may be due to a combination of the high symmetry of the phase plus the very localized character of the two groups of high-frequency modes, which could have acted as scattering channels if they had a greater overlap with those in the low-energy region.

3. Conclusions

To sum up, we characterize the ground state and phonon dispersions of four proposed arsenene structures (buckled, puckered, tricycle and square/octagon) with very different geometric features and degrees of structural complexity. Our analysis shows the tricycle structure to be unstable. Furthermore, the relative stability of the remaining three can only be correctly understood when phonons are taken into account, even at vanishing temperature. Specifically, we predict the puckered and s/o structures to be thermodynamically favored at low and high temperatures respectively, in contrast with previous assertions in the literature that the buckled phase would be the most stable. We then characterize also the anharmonic features of the three stable structures and compute their thermal conductivities from first principles. We show the two most complex structures to have high thermal conductivities due to a combination of harmonic and anharmonic features, which eludes simplistic interpretations in terms of unit cell complexity.

We expect our results to be of help to experimental efforts toward the synthesis of proposed arsenene structures. More generally, every conclusion from this study highlights the crucial role of an appropriate treatment of phonons in the equilibrium and transport thermodynamics of 2D systems. This can be expected to become more important as computational explorations of libraries of 2D materials become more elaborate, since more numerous, more complex and chemically richer structures can be expected to be put forward, demanding careful examination of their practical feasibility.

Acknowledgement

The authors acknowledge the support from the European Union’s Horizon 2020 Research and Innovation Programme [grant no. 645776 (ALMA)] and from the Xunta de Galicia (grants nos. AGRUP2015/11 and GRC ED431C 2016/001) in conjunction with the

European Regional Development Fund (FEDER). We also thank Dr. Amador García-Fuente for useful discussions. The computational results presented have been achieved in part using the Vienna Scientific Cluster (VSC).

References

- [1] Novoselov K S, Geim A K, Morozov S V, Jiang D, Zhang Y, Dubonos S V, Grigorieva I V and Firsov A A 2004 *Science* **306** 666–669
- [2] Wallace P R 1947 *Phys. Rev.* **71** 622–634
- [3] Reich S, Maultzsch J, Thomsen C and Ordejón P 2002 *Phys. Rev. B* **66** 035412
- [4] Novoselov K S, Jiang D, Schedin F, Booth T J, Khotkevich V V, Morozov S V and Geim A K 2005 *PNAS* **102** 10451–10453
- [5] Geim A K and Novoselov K S 2007 *Nat. Mater.* **6** 183–191
- [6] Castro Neto A H, Guinea F, Peres N M R, Novoselov K S and Geim A K 2009 *Rev. Mod. Phys.* **81** 109–162
- [7] Chen D, Tang L and Li J 2010 *Chem. Soc. Rev.* **39** 3157–3180
- [8] Das Sarma S, Adam S, Hwang E H and Rossi E 2011 *Rev. Mod. Phys.* **83** 407–470
- [9] Singh V, Joung D, Zhai L, Das S, Khondaker S I and Seal S 2011 *Prog. Mater. Sci.* **56** 1178–1271
- [10] Sun Y, Wu Q and Shi G 2011 *Energy Environ. Sci.* **4** 1113–1132
- [11] Huang Y, Liang J and Chen Y 2012 *Small* **8** 1805–1834
- [12] Wang Q H, Kalantar-Zadeh K, Kis A, Coleman J N and Strano M S 2012 *Nat. Nano.* **7** 699–712
- [13] Geim A K and Grigorieva I V 2013 *Nature* **499** 419–425
- [14] Butler S Z, Hollen S M, Cao L, Cui Y, Gupta J A, Gutiérrez H R, Heinz T F, Hong S S, Huang J, Ismach A F, Johnston-Halperin E, Kuno M, Plashnitsa V V, Robinson R D, Ruoff R S, Salahuddin S, Shan J, Shi L, Spencer M G, Terrones M, Windl W and Goldberger J E 2013 *ACS Nano* **7** 2898–2926
- [15] Xu M, Liang T, Shi M and Chen H 2013 *Chem. Rev.* **113** 3766–3798
- [16] Gupta A, Sakthivel T and Seal S 2015 *Prog. Mater. Sci.* **73** 44–126
- [17] Yan J A, Stein R, Schaefer D M, Wang X Q and Chou M Y 2013 *Phys. Rev. B* **88** 121403
- [18] Balog R, Jørgensen B, Nilsson L, Andersen M, Rienks E, Bianchi M, Fanetti M, Lægsgaard E, Baraldi A, Lizzit S, Sljivancanin Z, Besenbacher F, Hammer B, Pedersen T G, Hofmann P and Hornekær L 2010 *Nat. Mater.* **9** 315–319
- [19] Quhe R, Fei R, Liu Q, Zheng J, Li H, Xu C, Ni Z, Wang Y, Yu D, Gao Z and Lu J 2012 *Sci. Rep.* **2** 853
- [20] Ye M, Quhe R, Zheng J, Ni Z, Wang Y, Yuan Y, Tse G, Shi J, Gao Z and Lu J 2014 *Physica E: Low-dimensional Systems and Nanostructures* **59** 60–65
- [21] Mak K F, Lui C H, Shan J and Heinz T F 2009 *Phys. Rev. Lett.* **102** 256405
- [22] Ni Z, Liu Q, Tang K, Zheng J, Zhou J, Qin R, Gao Z, Yu D and Lu J 2012 *Nano Lett.* **12** 113–118
- [23] Liu H, Neal A T, Zhu Z, Luo Z, Xu X, Tománek D and Ye P D 2014 *ACS Nano* **8** 4033–4041
- [24] Li L, Yu Y, Ye G J, Ge Q, Ou X, Wu H, Feng D, Chen X H and Zhang Y 2014 *Nat. Nano.* **9** 372–377
- [25] Zhu Z and Tománek D 2014 *Phys. Rev. Lett.* **112** 176802
- [26] Zhang S, Yan Z, Li Y, Chen Z and Zeng H 2015 *Angew. Chem. Int. Ed.* **54** 3112–3115
- [27] Kamal C and Ezawa M 2015 *Phys. Rev. B* **91** 085423
- [28] Özçelik V O, Aktürk O U, Durgun E and Ciraci S 2015 *Phys. Rev. B* **92** 125420
- [29] Kecik D, Durgun E and Ciraci S 2016 *Phys. Rev. B* **94** 205409
- [30] Aktürk O U, Özçelik V O and Ciraci S 2015 *Phys. Rev. B* **91** 235446
- [31] Aktürk E, Aktürk O U and Ciraci S 2016 *Phys. Rev. B* **94** 014115
- [32] Ersan F, Aktürk E and Ciraci S 2016 *Phys. Rev. B* **94** 245417

- [33] Carrete J, Li W, Lindsay L, Broido D A, Gallego L J and Mingo N 2016 *Mater. Res. Lett.* **4** 204–211
- [34] Ma S, Zhou P, Sun L Z and Zhang K W 2016 *Phys. Chem. Chem. Phys.* **18** 8723–8729
- [35] Tsai H S, Wang S W, Hsiao C H, Chen C W, Ouyang H, Chueh Y L, Kuo H C and Liang J H 2016 *Chem. Mater.* **28** 425–429
- [36] Zeraati M, Vaez Allaei S M, Abdolhosseini Sarsari I, Pourfath M and Donadio D 2016 *Phys. Rev. B* **93** 085424
- [37] Zheng G, Jia Y, Gao S and Ke S H 2016 *Phys. Rev. B* **94** 155448
- [38] Li W, Carrete J, Katcho N A and Mingo N 2014 *Comp. Phys. Comm.* **185** 1747–1758
- [39] Kresse G and Hafner J 1993 *Phys. Rev. B* **47** 558–561
- [40] Kresse G and Hafner J 1994 *Phys. Rev. B* **49** 14251–14269
- [41] Kresse G and Furthmüller J 1996 *Comp. Mater. Sci.* **6** 15–50
- [42] Kresse G and Furthmüller J 1996 *Phys. Rev. B* **54** 11169–11186
- [43] Blöchl P E 1994 *Phys. Rev. B* **50** 17953–17979
- [44] Kresse G and Joubert D 1999 *Phys. Rev. B* **59** 1758–1775
- [45] Perdew J P, Burke K and Ernzerhof M 1996 *Phys. Rev. Lett.* **77** 3865–3868
- [46] Perdew J P, Burke K and Ernzerhof M 1997 *Phys. Rev. Lett.* **78** 1396–1396
- [47] Togo A and Tanaka I 2015 *Scr. Mater.* **108** 1–5
- [48] Smith B, Vermeersch B, Carrete J, Ou E, Kim J, Mingo N, Akinwande D and Shi L 2017 *Adv. Mater.* **29**
- [49] Tamura S i 1983 *Phys. Rev. B* **27** 858–866
- [50] Vermeersch B, Carrete J and Mingo N 2016 *Appl. Phys. Lett.* **108** 193104
- [51] Carrete J, Mingo N, Wang S and Curtarolo S 2014 *Adv. Funct. Mater.* **24** 7427–7432